Naunyn-Schmiedeberg's Arch Pharmacol (2015) 388:1039–1052
DOI 10.1007/s00210-015-1133-2

ORIGINAL ARTICLE

Flow cytometric analysis with a fluorescently labeled formyl peptide receptor ligand as a new method to study the pharmacological profile of the histamine H_2 receptor

Kristin Werner[1] · Solveig Kälble[1] · Sabine Wolter[1] · Erich H. Schneider[1] · Armin Buschauer[2] · Detlef Neumann[1] · Roland Seifert[1]

Received: 16 January 2015 / Accepted: 18 May 2015 / Published online: 30 May 2015

Abstract The histamine H_2 receptor (H_2R) is a G_s protein-coupled receptor. Its activation leads to increases in the second messenger adenosine-3′,5′-cyclic monophosphate (cAMP). Presently, several systems are established to characterize the pharmacological profile of the H_2R, mostly requiring radioactive material, animal models, or human blood cells. This prompted us to establish a flow cytometric analysis with a fluorescently labeled formyl peptide receptor (FPR) ligand in order to investigate the H_2R functionally and pharmacologically. First, we stimulated U937 promonocytes, which mature in a cAMP-dependent fashion upon H_2R activation, with histamine (HA) or selective H_2R agonists and measured increases in cAMP concentrations by mass spectrometry. Next, indicative for the maturation of U937 promonocytes, we assessed the FPR expression upon incubation with HA or H_2R agonists. FPR expression was measured either indirectly by formyl peptide-induced changes in intracellular calcium concentrations ($[Ca^{2+}]_i$) or directly with the fluorescein-labeled FPR ligand fNleLFNleYK-Fl. HA and H_2R agonists concentration-dependently induced FPR expression, and potencies and efficacies of fMLP-induced increases in $[Ca^{2+}]_i$ and FPR density correlated linearly. Accordingly, flow cytometric analysis of FPR expression constitutes a simple, inexpensive, sensitive, and reliable method to characterize the H_2R pharmacologically. Furthermore, we evaluated FPR expression at the mRNA level. Generally, quantitative real-time polymerase chain reaction confirmed functional data. Additionally, our study supports the concept of functional selectivity of the H_2R, since we observed dissociations in the efficacies of HA and H_2R agonists in cAMP accumulation and FPR expression.

Keywords Histamine H_2 receptor · Formyl peptide receptor · Functional selectivity · U937 promonocytes

Abbreviations

AC	Adenylyl cyclase
ACTB	ß-actin
AM	Amthamine
$[Ca^{2+}]_i$	Intracellular calcium concentration
cAMP	Adenosine-3′,5′-cyclic monophosphate
C5aR	C5a receptor
DB-cAMP	N^6,2′-*O*-dibutyryladenosine-3′,5′-cyclic monophosphate
DI	Dimaprit
FAM	Famotidine
fMLP	*N*-formyl-L-methionyl-L-leucyl-L-phenylalanine
fNleLFNleYK-Fl	Fluorescein-labeled formyl-Nle-Leu-Phe-Nle-Tyr-Lys
FPR	Formyl peptide receptor
GPCR	G protein-coupled receptor
GUSB	ß-glucuronidase

Electronic supplementary material The online version of this article (doi:10.1007/s00210-015-1133-2) contains supplementary material, which is available to authorized users.

✉ Roland Seifert
seifert.roland@mh-hannover.de

[1] Institute of Pharmacology, Hannover Medical School, Carl-Neuberg-Straße 1, 30625 Hannover, Germany

[2] Department of Pharmaceutical and Medicinal Chemistry II, University of Regensburg, 93040 Regensburg, Germany

HA	Histamine
H_2R	Histamine H_2 receptor
IBMX	3-Isobutyl-1-methylxanthine
IM	Impromidine
JNJ	1-[(5-Chloro-1H-indol-2-yl) carbonyl]-4-methylpiperazine (JNJ7777120)
MEP	Mepyramine
Nle	Norleucine
UR-NK22	(1-(Amino{[3-(2-amino-4-methyl-thiazol-5-yl)propyl]amino} methylene)-3-{6-[3-(amino{[3-(2-amino-4-methyl-thiazol-5-yl)propyl]amino}methylene) ureido]hexyl}urea)
PCR	Polymerase chain reaction
PROB	Probenecid
ROL	Rolipram
ROS	Reactive oxygen species
TIO	Tiotidine
5-MHA	5-Methylhistamine

Introduction

Canonically, the histamine H_2 receptor (H_2R) belongs to the family of G protein-coupled receptors (GPCR) and couples to G_s proteins. Binding of the endogenous ligand histamine (HA) results in activation of adenylyl cyclases (AC) followed by increases in adenosine-3′,5′-cyclic monophosphate (cAMP) (Seifert et al. 2013). However, the classic two-state model describing GPCR activation has been substituted by a multiple-state model also referred to as functional selectivity. This concept states that each ligand stabilizes a unique receptor-conformation leading to activation of not only G protein-dependent but also G protein-independent signaling in a ligand-dependent manner (Azzi et al. 2003, Kenakin 2012, Seifert 2013, Urban et al. 2007). We previously noticed deviations in H_2R-mediated cAMP generation and inhibition of fMLP-induced production of reactive oxygen species (ROS) in human monocytes supporting the concept of functional selectivity (Werner et al. 2014b). The H_2R has been of clinical importance for many years, e.g., H_2R antagonists inhibit H^+ secretion in parietal cells and are applied to treat acid-induced gastrointestinal diseases (Hershcovici and Fass 2011). Additionally, HA (Ceplene®), approved as an orphan drug in the postconsolidation therapy of patients suffering from acute myeloid leukemia (AML), exerts its anti-leukemic effect exclusively via H_2R (Martner et al. 2010). Therefore, there is considerable interest in the development of a new class of potent and selective H_2R agonists (Birnkammer et al. 2012, Kagermeier et al. 2015).

Several research groups have used U937 promonocytes in order to characterize the H_2R (Gespach et al. 1985, Shayo et al. 1997, Smit et al. 1994). In the 1980s, Gespach et al. already assumed that the H_2R is involved in U937 cell maturation (Gespach et al. 1985). Interestingly, the AC activator forskolin as well as the cAMP analog DB-cAMP induced cell maturation in U937 promonocytes, whereas neither HA nor H_2R agonists did so. According to Shayo et al., lack of differentiation was related to H_2R desensitization (Brodsky et al. 1998, Shayo et al. 1997). By contrast, targeting the H_2R on HL-60 promyelocytes resulted in cell differentiation (Sawutz et al. 1984, Seifert et al. 1992). Recently, Copsel et al. reported on U937 cell differentiation via H_2R. In their study, the H_2R agonist amthamine (AM) induced cell maturation in the presence of the phosphodiesterase inhibitor rolipram (ROL) and the multidrug resistance-associated protein inhibitor probenecid (PROB) (Copsel et al. 2011). Cell maturation of U937 cells can be analyzed by evaluation of formyl peptide receptor (FPR) expression (Kay et al. 1983). The FPR is a G_i protein-coupled receptor. Binding of the bacterial peptide *N*-formyl-L-methionyl-L-leucyl-L-phenylalanine (fMLP) leads to activation of phospholipase C and, subsequently, increases in intracellular calcium concentrations ($[Ca^{2+}]_i$) (Wenzel-Seifert et al. 1998).

In our present study, we characterized the pharmacological profile of the H_2R with HA and various selective H_2R agonists, including the new bivalent H_2R agonist UR-NK22 (Kagermeier et al. 2015). The chemical structures are shown in Fig. 1. First, we analyzed cAMP accumulation caused by HA or H_2R ligands. Second, we differentiated U937 promonocytes with HA or H_2R ligands in the presence of both the phosphodiesterase inhibitor 3-isobutyl-1-methylxanthine (IBMX) and PROB and assessed FPR expression. In addition to measuring fMLP-induced rises in $[Ca^{2+}]_i$, we established a flow cytometric assay with a fluorescein-labeled FPR ligand. Moreover, we assessed FPR expression at the mRNA level by quantitative real-time polymerase chain reaction (PCR). Finally, we compared potencies and efficacies of HA and H_2R agonists in all three assays in order to verify the concept of functional selectivity. Thereby, we evaluated the use of the fluorescent FPR ligand as a new approach to study H_2R function and pharmacology.

Materials and methods

Materials

Histamine dihydrochloride (HA); amthamine dihydrobromide (AM); dimaprit dihydrochloride (DI); JNJ7777120 (1-[(5-chloro-1H-indol-2-yl)carbonyl]-4-methylpiperazine, herein referred to as JNJ); mepyramine maleate (MEP); 5-methylhistamine dihydrochloride (5-MHA); and Fura-2 AM

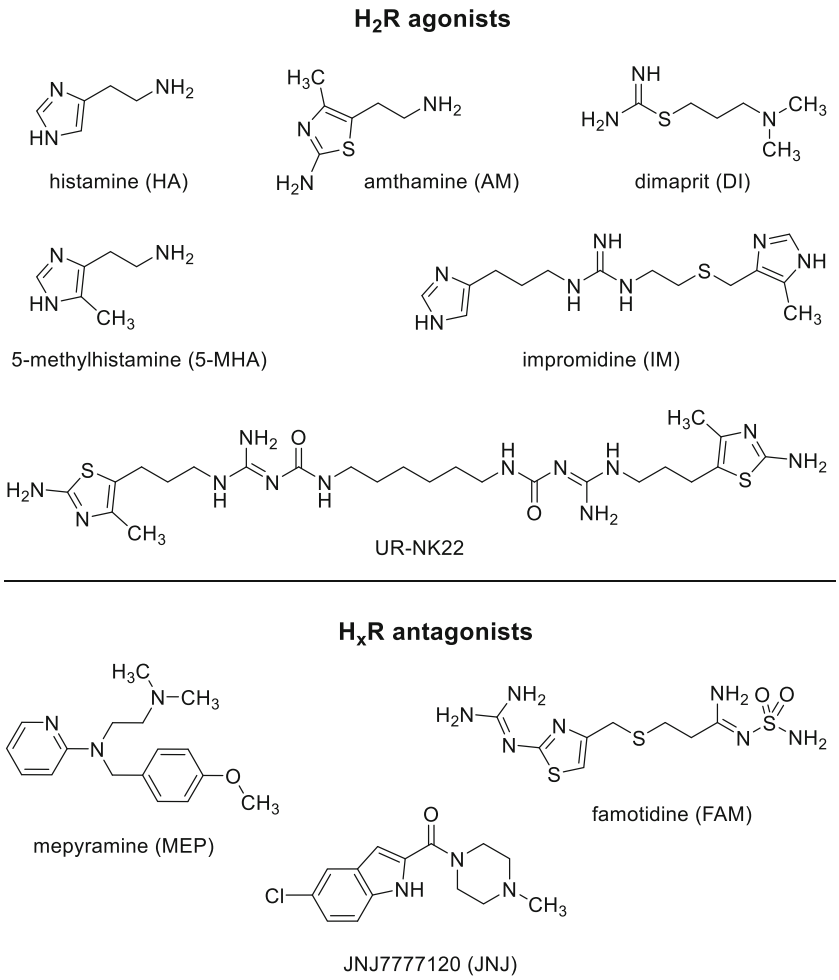

Fig. 1 Chemical structures of histamine receptor ligands

were obtained from Tocris Bioscience (Bristol, UK). Impromidine (IM) and UR-NK22 ((1-(Amino{[3-(2-amino-4-methyl-thiazol-5-yl)propyl]amino}methylene)-3-{6-[3-(amino{[3-(2-amino-4-methyl-thiazol-5-yl)propyl]amino}methylene)ureido]hexyl}urea)) (Kagermeier et al. 2015) were synthesized at the University of Regensburg. 3-Isobutyl-1-methylxanthine (IBMX), probenecid (PROB), *N*-formyl-L-methionyl-L-leucyl-L-phenylalanine (fMLP), famotidine (FAM), Triton X-100, RPMI-1640 medium, bovine calf serum, L-glutamine, and penicillin-streptomycin (10,000 U/ml; 10 mg/ml) were purchased from Sigma Aldrich (St. Louis, MO, USA). EGTA was obtained from Fluka (Deisenhofen, Germany). Minimum Eagle's medium nonessential amino acid solution (100×) (NEA) and 10× Dulbecco's phosphate-buffered saline (PBS) without Ca^{2+} and Mg^{2+} were supplied by PAA Laboratories (Pasching, Austria). Fluorescein-labeled *N*-formyl-Nle-Leu-Phe-Nle-Tyr-Lys (fNleLFNleYK-Fl) (lot no. 1,212,098) was purchased from Life Technologies (Darmstadt, Germany). N^6,2′-*O*-dibutyryl adenosine-3′,5′-cyclic monophosphate (DB-cAMP) was from BIOLOG (Bremen, Germany). Stock solutions (10 mM) of HA, AM, DI, 5-MHA, IM, UR-NK22, FAM and IBMX were prepared in distilled water and stock solutions (10 mM) of MEP, JNJ, and fMLP in dimethylsulfoxide. PROB (100 mM) and DB-cAMP (200 mM) were also dissolved in dimethylsulfoxide. Tenofovir was from the National Institutes of Health (Bethesda, MD, USA). RevertAid M-MuLV Reverse Transcriptase (200 U/μl), oligo$(dT)_{18}$ primer, random hexamer primer, dNTP mix (10 mM), and 5× Reaction Buffer were purchased from Fermentas (St. Leon-Rot, Germany). RiboLock RNAse Inhibitor (40 U/μl) was supplied by Thermo Scientific (Wilmington, DE, USA). TaqMan probes (Hs00939627_m1 (GUSB) LOT#1,191,192, Hs99999903_m1 (ACTB) LOT#1,191,192, Hs04235426_s1 (FPR1) LOT#4,448,892, Hs01912307_s1 (FPR1) LOT#4, 331,182) and TaqMan Gene Expression Master Mix were purchased from Applied Biosystems (Darmstadt, Germany). All other chemicals were obtained from standard sources.

Culture of U937 promonocytes

U937 cells were obtained from the American Type Culture Collection (ATCC, Manassas, VA, USA). Cells were cultured in RPMI-1640 medium supplemented with 10 % (*v*/*v*) bovine

calf serum, 2 mM L-glutamine, 100 U/ml penicillin, 100 μg/ml streptomycin, and 1 % (*v*/*v*) nonessential amino acid solution at 37 °C in a humidified atmosphere with 5 % (*v*/*v*) CO_2. Cells were maintained at a density of 0.05–1 × 10^6 cells/ml.

Quantification of cAMP levels

In order to assess the effects of IBMX, PROB, and HA on intracellular cAMP ($cAMP_{intra}$) concentrations, 50-μl aliquots containing different combinations of 2× concentrated IBMX (200 μM), PROB (1 mM), and HA (20 μM) in PBS, supplemented with 2× concentrated $CaCl_2$ (2 mM), were preincubated at 37 °C for 5 min. U937 cells were resuspended in PBS at a density of 5 × 10^6 cells/ml. Reactions were initiated by adding 50 μl of cell suspension to the premixed and warmed 2× concentrated reagents in 2-ml safe-lock tubes. Following incubation at 37 °C for 10 min, cells were diluted with 1 ml of ice-cold 1× PBS and centrifuged at 300×*g* and 4 °C for 5 min. Thereafter, the supernatant fluids were discarded, the cell pellet resuspended in 100 μl of 1× PBS, and the samples heated at 95 °C for 10 min.

For concentration-response curves of HA and H_2R agonists, total cAMP levels were determined. Therefore, 50-μl aliquots of PBS, supplemented with 2× concentrated IBMX (200 μM) and $CaCl_2$ (2 mM), were preincubated with ligands at different concentrations at 37 °C for 5 min. U937 cells (5 × 10^6 cells/ml) were resuspended in PBS, and 50 μl of cell suspension were added to the premixed and warmed 2× concentrated reagents in 2-ml safe-lock tubes followed by a 10-min exposure at 37 °C. To stop the reactions, tubes were placed on ice and subsequently heated at 95 °C for 10 min. Experiments with H_xR antagonists were conducted in an analogous manner.

Finally, all samples were cooled down on ice and 100 μl of ice-cold eluent A (3/97 MeOH/H_2O, 50 mM NH_4OAc, 0.1 % (*v*/*v*) HOAc) with tenofovir (100 ng/ml) as internal standard were added to each sample. Tubes were centrifuged at 10,000×*g* and 4 °C for 10 min. The analysis of cAMP levels in supernatants was performed via reversed phase HPLC-coupled mass spectrometry (HPLC-MS/MS) as described (Brunskole Hummel et al. 2013).

Differentiation of U937 promonocytes

For cell differentiation, U937 cells were seeded in 12-well plates at a density of 3 × 10^5 cells/ml and exposed to various stimuli in a humidified atmosphere at 37 °C with 5 % (*v*/*v*) CO_2 for 24 h. Differentiation with HA or H_2R agonists was performed in the presence of 100 μM IBMX and 500 μM PROB. After 24 h, cell numbers were determined using the MACSQuant Analyzer (Miltenyi Biotec, Bergisch-Gladbach, Germany).

Measurement of fMLP-induced $[Ca^{2+}]_i$

Changes in $[Ca^{2+}]_i$ were determined by the Fura-2 AM method as previously described (Werner et al. 2014a). Briefly, 2.5 × 10^5 U937 cells were resuspended in 500 μl of assay buffer (138 mM NaCl, 6 mM KCl, 1 mM $MgSO_4$,1 mM Na_2HPO_4, 5 mM $NaHCO_3$, 5.5 mM D-(+)-glucose, 20 mM HEPES, and 0.1 % (*w*/*v*) bovine serum albumin, pH 7.4) and incubated in the presence of 4 μM Fura-2 AM at 37 °C and 5 % (*v*/*v*) CO_2 for 10 min, followed by dilution (1:2) with assay buffer and incubation for an additional 45 min. Subsequently, cells were diluted with 9 ml of assay buffer and centrifuged at 300×*g* and 4 °C for 5 min. The supernatant was discarded and 2.5 × 10^5 cells were resuspended in 2 ml of assay buffer supplemented with 1 mM $CaCl_2$. Fluorescence (excitation wavelength, 340 nm; emission wavelength, 508 nm) was measured at 37 °C under constant stirring with a Shimadzu RF 5301 fluorescence spectrometer (Shimadzu, Duisburg, Germany). Basal fluorescence was determined for 1 min, and, subsequently, 1 μM fMLP was added to samples and fluorescence signals were recorded for 2 min. In order to assess $[Ca^{2+}]_i$, each sample was calibrated by measuring the maximum fluorescence signal (F_{max}) after the addition of Triton X-100 to a final concentration of 0.5 % (*v*/*v*) and the minimum fluorescence signal (F_{min}) in the presence of 12 mM EGTA. $[Ca^{2+}]_i$ was calculated according to the following equation: $[Ca^{2+}]_i = K_d \times [(F - F_{min})/(F_{max} - F)]$ (Grynkiewicz et al. 1985).

FPR expression

FPR expression was analyzed by flow cytometry. 1 × 10^6 U937 cells/ml were resuspended in a binding buffer (pH 7.4) consisting of Hank's balanced salt solution (HBSS) supplemented with 0.1 % (*w*/*v*) bovine serum albumin and 20 mM HEPES and kept on ice until use. For fluorescent labeling, the fluorescein-labeled FPR ligand fNleLFNleYK-FI (emission maximum, 516 nm) was applied. To determine nonspecific fNleLFNleYK-FI binding, cells were treated with fNleLFNleYK-FI in the presence (nonspecific binding) or absence (total binding) of fMLP. Seventy-five microliters of binding buffer containing 2× concentrated fNleLFNleYK-FI (final 50 nM) (with or without 2× concentrated fMLP (final 50 μM)) were pipetted into a well of a 96-well plate. After adding 75 μl of cell suspension, cells were incubated for 45 min on ice in the dark. Fluorescent cells were analyzed with the MACSQuant Analyzer (Miltenyi Biotec).

Quantitative real-time polymerase chain reaction

FPR1 expression was assessed at the mRNA level via quantitative real-time PCR as described (Werner et al. 2014b). Data were analyzed using the $2^{-\Delta\Delta C(T)}$ method (Livak and

Schmittgen 2001) with human ß-glucuronidase (GUSB) and ß-actin (ACTB), respectively, serving as housekeeping genes.

Statistics

All data are reported as means ± SEM obtained from at least three independent experiments performed in singles to triplicates. The experiments were evaluated using GraphPad Prism software version 5.01 (San Diego, CA, USA). Concentration-response curves were analyzed by nonlinear regression. Statistical significance was determined by one-way ANOVA followed by Dunnett's multiple comparison test with ***$p < 0.001$, **$p < 0.01$, and *$p < 0.05$.

Results

Effect of HA and selective H_2R agonists on cAMP accumulation in U937 promonocytes

In order to determine whether HA induces intracellular cAMP accumulation ($cAMP_{intra}$), we first quantified changes in $cAMP_{intra}$ concentration after incubation with HA (10 μM) for 10 min (Fig. 2a). Next, we evaluated whether the addition of either IBMX (100 μM) or PROB (500 μM) enhances $cAMP_{intra}$. Compared to the increase induced by HA alone, combinations of HA plus IBMX as well as HA, IBMX plus PROB showed significantly higher $cAMP_{intra}$, whereas the addition of PROB alone to HA did not result in significant changes. Treatment with IBMX, PROB, or IBMX plus PROB in the absence of HA did not induce changes in $cAMP_{intra}$ compared to basal level (PBS) (Fig. 2a). In order to prove that HA causes cAMP accumulation exclusively via the H_2R, U937 promonocytes were treated with HA in the presence of H_xR-selective antagonists. While FAM (10 μM; H_2R antagonist) inhibited the effect of HA, neither MEP (1 μM; H_1R antagonist) nor JNJ (1 μM; H_4R antagonist) did so (Fig. 2b). Next, we constructed concentration-response curves for HA, AM, DI, 5-MHA, IM, and UR-NK22, ranging from 1 nM to 100 μM, in the presence of IBMX (100 μM) and analyzed the data by nonlinear regression (Fig. 3a–f). The calculated potencies and efficacies are summarized in Table 1.

HA and selective H_2R agonists induce FPR expression on U937 cells

Stimulation of undifferentiated U937 promonocytes with fMLP (1 μM) did not result in increases in $[Ca^{2+}]_i$ (Fig. 4a). Incubation with HA (100 μM) for 24 h and subsequent stimulation with fMLP (1 μM) showed a small increase in $[Ca^{2+}]_i$ (Fig. 4b). This signal was enhanced in the presence of IBMX (100 μM) or PROB (500 μM), and combination of HA, IBMX plus PROB resulted in a maximal signal of fMLP-induced $[Ca^{2+}]_i$ (Fig. 4c–e). By contrast, treatment with IBMX or PROB alone and in combination did not induce increases in $[Ca^{2+}]_i$ (Fig. 4f–h). Based on these results, IBMX and PROB were added to each sample in order to assess FPR expression and function caused by HA or H_2R agonists. Next, we constructed concentration-response curves of HA, AM, DI, 5-MHA, IM, and UR-NK22 in the presence

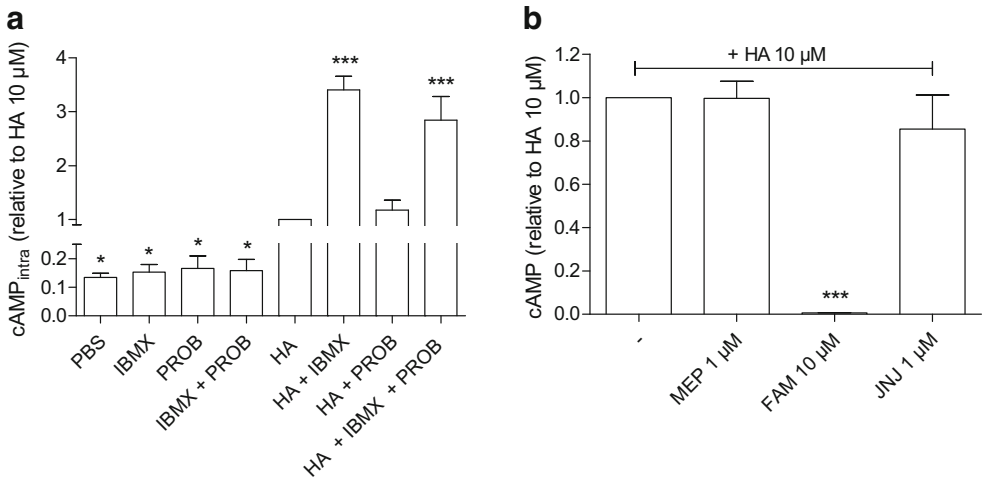

Fig. 2 Evaluation of cAMP concentrations. **a** U937 promonocytes were stimulated with different combinations of HA (10 μM), IBMX (100 μM), and PROB (500 μM) for 10 min. **b** Cells were incubated with HA (10 μM) alone and in the presence of the H_xR antagonists MEP (1 μM), FAM (10 μM), or JNJ (1 μM) for 10 min. Data were normalized to the effect of HA (10 μM). Analysis of cAMP levels was conducted as described in the "Materials and methods" section. Values represent means ± SEM from three independent experiments performed in triplicate. Statistical significance was calculated using one-way ANOVA followed by Dunnett's multiple comparison test with HA (10 μM) serving as reference (***$p < 0.001$ and *$p < 0.05$)

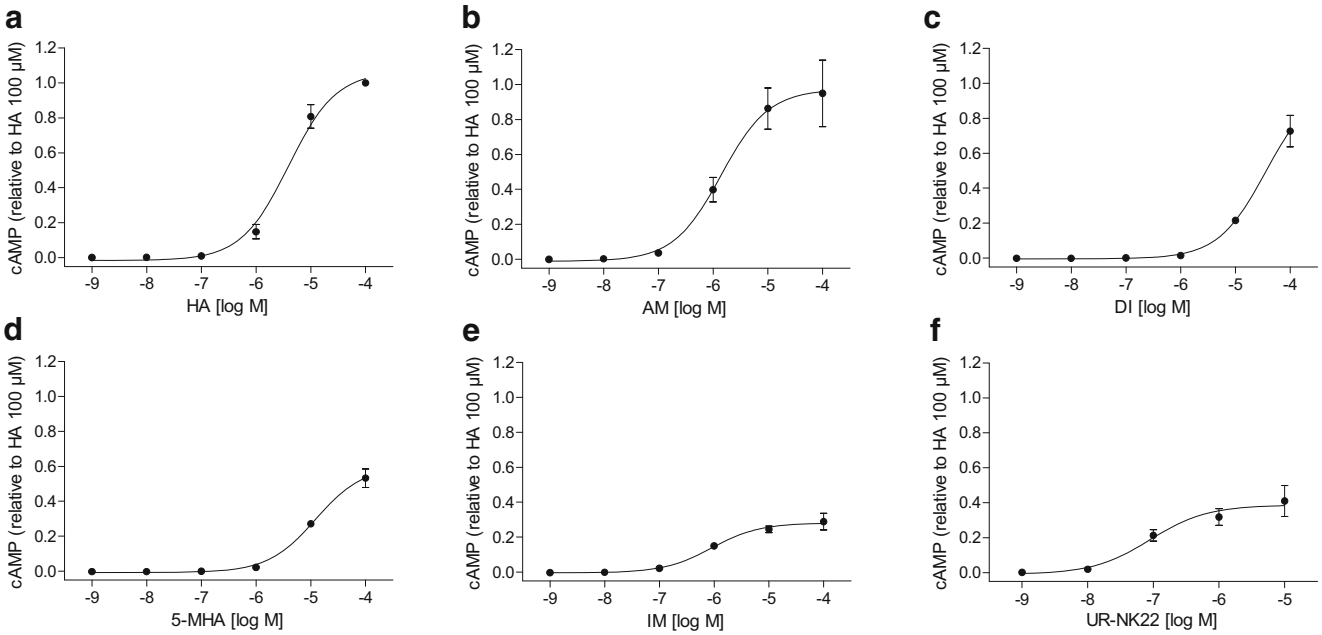

Fig. 3 Concentration-response curves of HA and selective H_2R agonists for cAMP accumulation. Determination of cAMP concentrations was carried out as described in the "Materials and methods" section. Data were normalized to the effect of HA (100 μM) and display means ± SEM from three independent experiments performed in triplicate

of IBMX and PROB by nonlinear regression analysis (Fig. 5a–f). Remarkably, the value of 100 μM DI was much smaller than the value obtained with 10 μM DI and, consequently, was excluded from nonlinear regression analysis. The calculated potencies and efficacies are shown in Table 1. Besides fMLP-induced $[Ca^{2+}]_i$, we evaluated FPR expression by flow cytometry. In order to assess nonspecific binding, the fluorescein-labeled ligand fNleLFNleYK-FI was displaced by fMLP. Therefore, we initially incubated U937 cells with DB-cAMP (400 μM) for 24 h and generated a competitive binding curve of fMLP ranging from 1 nM to 100 μM (Fig. 6a).

In the following experiments, we used fMLP at a concentration of 50 μM, which displaced 69 % of the specifically bound fNleLFNleYK-FI. Co-treatment of U937 cells with HA (10 μM) and H_xR antagonists revealed that FAM (10 μM; H_2R antagonist) inhibited FPR expression significantly ($p < 0.001$), whereas MEP (1 μM; H_1R antagonist) did not. Contrary to our expectations, JNJ (1 μM; H_4R antagonist) also inhibited FPR expression significantly ($p < 0.05$) (Fig. 6b). However, we previously reported that the H_4R is absent on U937 promonocytes as well as on human monocytes (Werner et al. 2014a). Likely, the effect of JNJ (1 μM) is attributable to

Table 1 Comparison of potencies and efficacies of HA and H_2R agonists in U937 promonocytes obtained from three different assays

	cAMP assay		fMLP-induced $[Ca^{2+}]_i$		FPR expression	
	pEC_{50} ± SEM	E_{max} ± SEM	pEC_{50} ± SEM	E_{max} ± SEM	pEC_{50} ± SEM	E_{max} ± SEM
HA	5.41 ± 0.08	1.00 ± 0.04	5.61 ± 0.13	1.00 ± 0.06	5.60 ± 0.19	1.00 ± 0.09
AM	5.85 ± 0.19	0.91 ± 0.08	6.48 ± 0.21**	1.18 ± 0.11	5.70 ± 0.17	1.16 ± 0.09
DI	–[a]	–[a]	–[a]	–[a]	5.47 ± 0.22	1.48 ± 0.15**
5-MHA	4.92 ± 0.08	0.56 ± 0.03***	5.53 ± 0.09	1.33 ± 0.06	5.44 ± 0.13	1.35 ± 0.08
IM	6.04 ± 0.15*	0.26 ± 0.02***	6.85 ± 0.19***	0.91 ± 0.08	6.92 ± 0.25***	0.76 ± 0.10
UR-NK22	7.05 ± 0.26***	0.37 ± 0.05***	7.17 ± 0.20***	0.89 ± 0.09	7.39 ± 0.18***	0.92 ± 0.08

cAMP accumulation, fMLP-induced $[Ca^{2+}]_i$, and FPR expression were assessed as described in the "Materials and methods" section. Potencies (pEC_{50}) and efficacies (E_{max}) were calculated from concentration-response curves obtained from nonlinear regression analysis as described in Figs. 3, 5, and 7. Efficacies are relative to the maximal effect of HA. Statistical significance was calculated using one-way ANOVA followed by Dunnett's multiple comparison test with HA serving as reference (***$p < 0.001$, **$p < 0.01$, and *$p < 0.05$)

[a] Saturation was not achieved at concentrations up to 100 μM DI

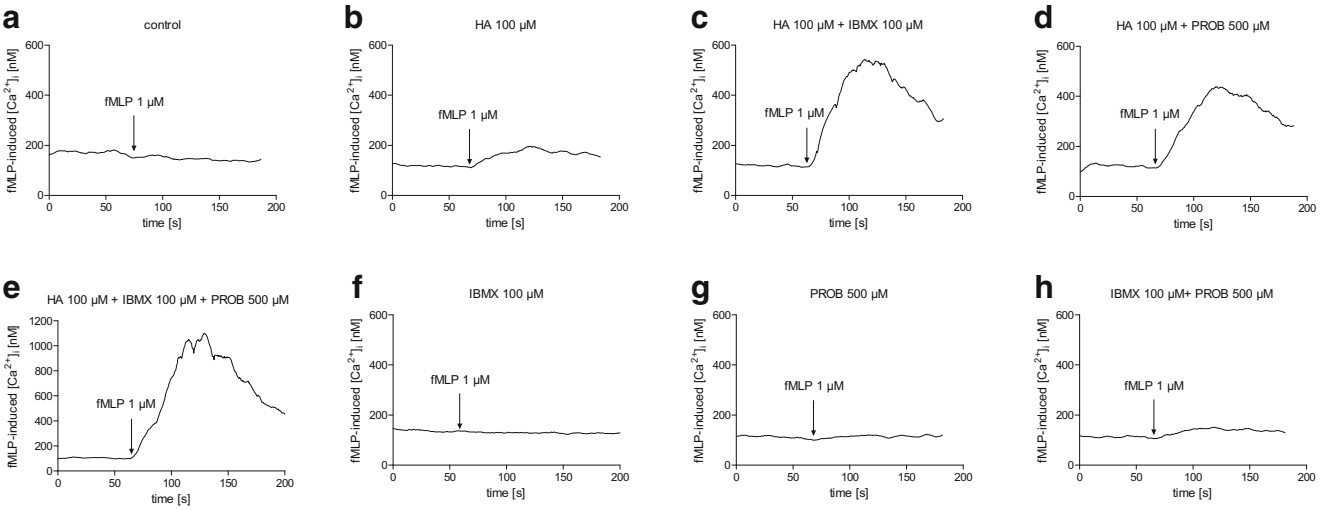

Fig. 4 Effects of IBMX, PROB, and HA on fMLP-induced $[Ca^{2+}]_i$. U937 promonocytes were incubated with different combinations of HA (100 μM), IBMX (100 μM), and PROB (500 μM) for 24 h. Subsequently, U937 cells were stimulated with fMLP (1 μM) and changes in $[Ca^{2+}]_i$ were recorded as described in the "Materials and methods" section. Results were confirmed in three independent evaluations. Please note the varied *y*-axis on Fig. 3e

a H_4R-independent nonspecific effect. HA, AM, DI, 5-MHA, IM, and UR-NK22 concentration-dependently induced FPR expression on U937 cells (Fig. 7a–f). In contrast to fMLP-induced increases in $[Ca^{2+}]_i$, 100 μM of DI strongly increased FPR expression as expected. Possibly, this relates to an H_2R-independent effect caused by a disulfide breakdown product as it has been described once before (Fechner et al. 1994). The calculated potencies and efficacies of HA and H_2R agonists are depicted in Table 1.

In addition, FPR1 mRNA expression was analyzed by quantitative real-time PCR with the FPR1 TaqMan probes Hs04235426_s1 (Fig. 8a and b) and Hs01912307_s1 (Fig. 8c, d), respectively. Unstimulated U937 promonocytes (control) hardly expressed FPR1 at the mRNA level. After

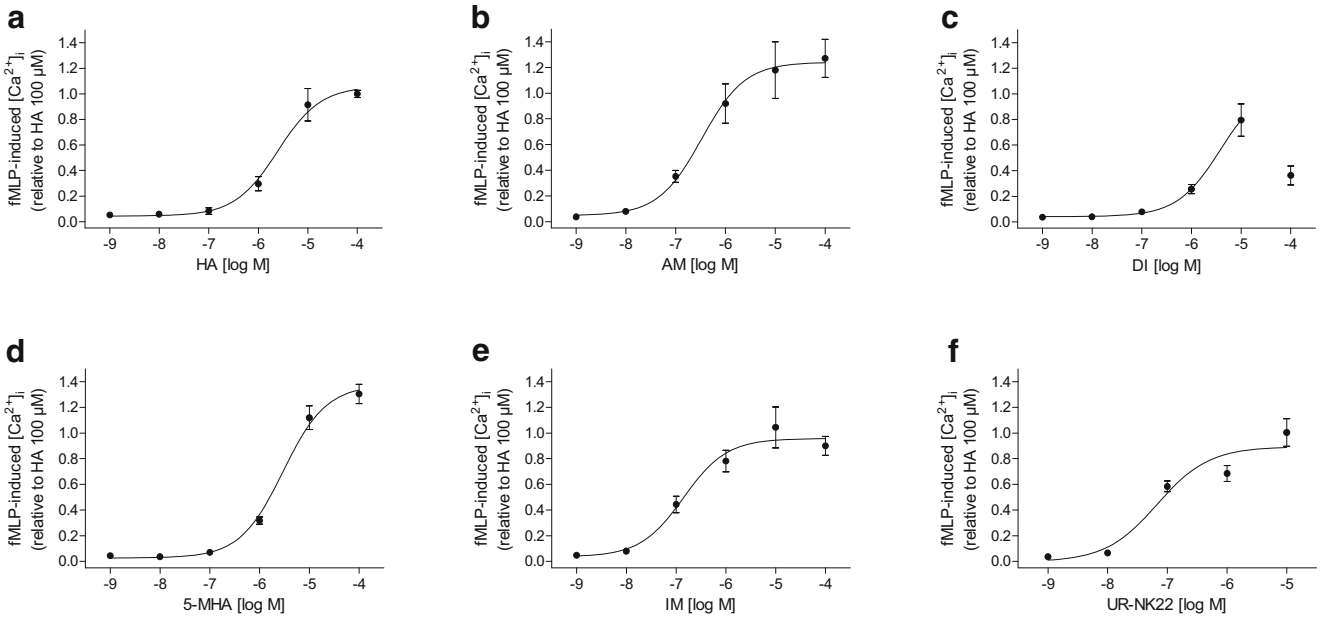

Fig. 5 Concentration-response curves of HA and selective H_2R agonists for fMLP-induced $[Ca^{2+}]_i$. U937 promonocytes were incubated with HA or selective H_2R agonists in the presence of IBMX (100 μM) and PROB (500 μM) for 24 h. Determination of fMLP-induced $[Ca^{2+}]_i$ was carried out as described in the "Materials and methods" section. Data were normalized to the effect of HA (100 μM) and represent means ± SEM from three independent evaluations

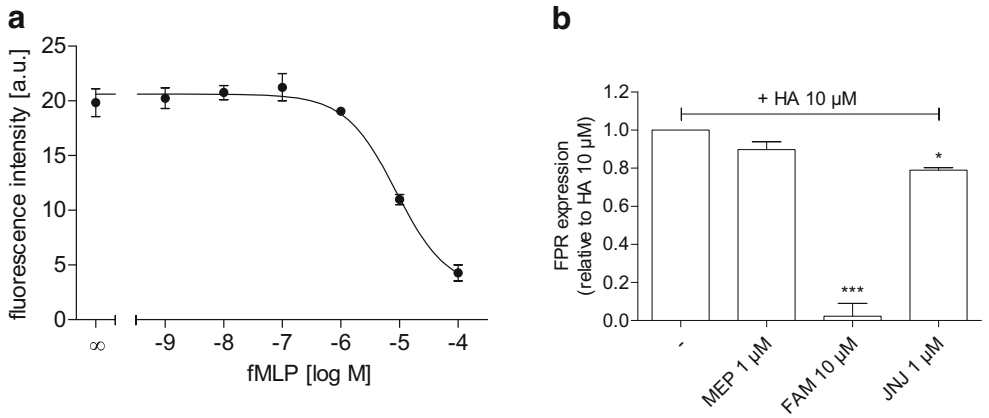

Fig. 6 Evaluation of FPR expression on U937 cells via flow cytometric analysis. **a** Competitive binding curve of fMLP for FPR expression. U937 promonocytes were incubated with DB-cAMP (400 µM) for 24 h. Fluorescence intensity was measured after exposure to different concentrations of fMLP (1 nM–100 µM), whereas the concentration of the fluorescence ligand fNleLFNleYK-FI (50 nM) remained constant. **b** Effects of H_xR antagonists on HA-induced FPR expression. Cells were incubated with HA (10 µM), IBMX (100 µM), and PROB (500 µM) alone and in combination with the H_xR antagonists MEP (1 µM), FAM (10 µM), or JNJ (1 µM) for 24 h. Data were normalized to the effect of HA (10 µM). FPR expression assay was performed as described in the "Materials and methods" section. Data are expressed as means ± SEM from three independent experiments performed in duplicate. Statistical significance was calculated using one-way ANOVA followed by Dunnett's multiple comparison test with HA (10 µM) serving as reference (***$p < 0.001$ and *$p < 0.05$)

exposure to HA (100 µM) for 24 h, small quantities of FPR1 mRNA were detectable which markedly increased in the presence of IBMX (100 µM) or PROB (500 µM). Treatment with PROB alone induced a considerable increase in FPR1 mRNA expression compared to control cells, whereas IBMX alone or the combination of IBMX and PROB had no or minimal effects on FPR1 expression. Co-treatment with HA and PROB resulted in higher FPR1 expression levels than HA and IBMX. Triple combination of HA, IBMX, and PROB showed FPR1 mRNA expression levels similar to HA and PROB. Notably, application of the FPR1 TaqMan probe Hs04235426_s1 resulted in about 10-fold higher FPR1 mRNA expression levels relative to control cells than the FPR1 TaqMan probe Hs01912307_s1.

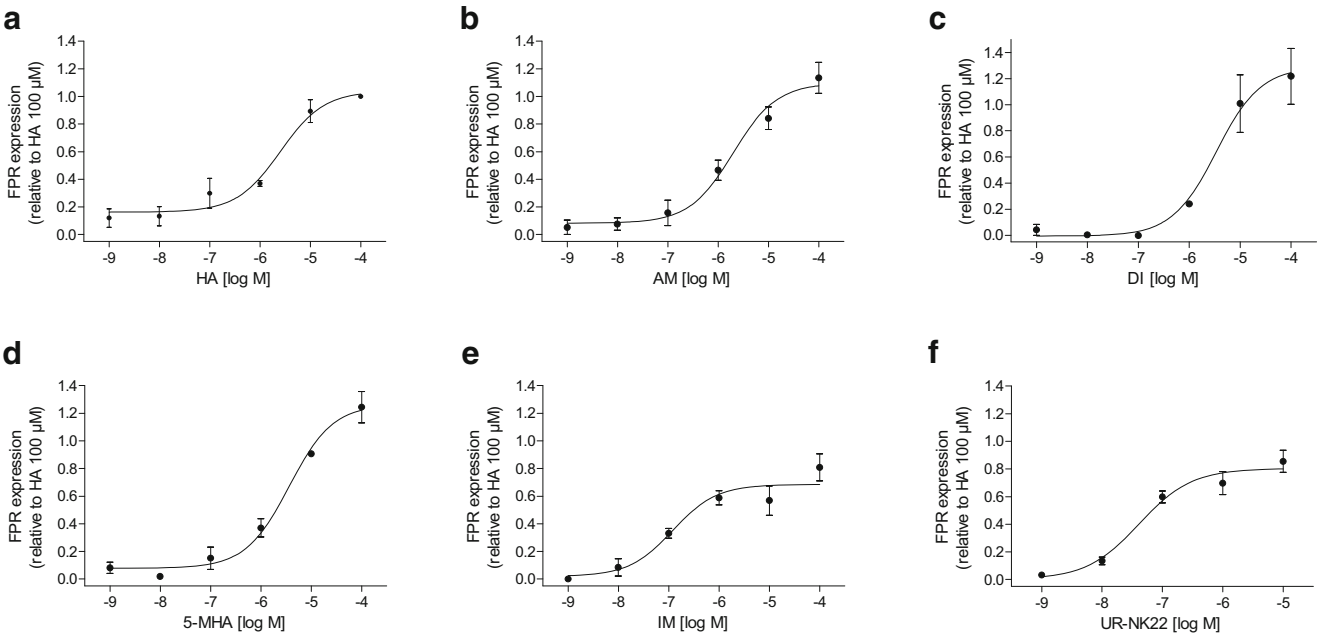

Fig. 7 Concentration-response curves of HA and selective H_2R agonists for FPR expression. U937 promonocytes were incubated with HA or selective H_2R agonists in the presence of IBMX (100 µM) and PROB (500 µM) for 24 h. Analysis of FPR expression was carried out as described in the "Materials and methods" section. Data were normalized to the effect of HA (100 µM) and represent means ± SEM from three independent experiments performed in duplicate

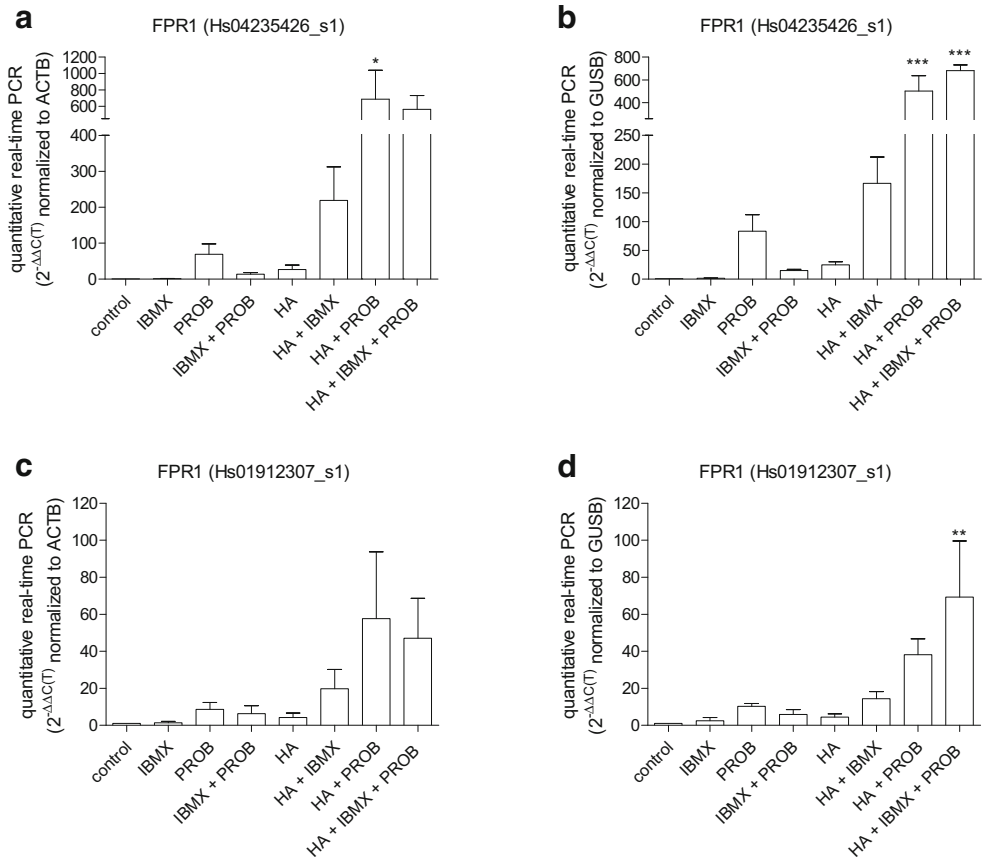

Fig. 8 Effects of IBMX, PROB, and HA on FPR1 expression at the mRNA level. U937 promonocytes were incubated with different combinations of HA (100 μM), IBMX (100 μM), and PROB (500 μM) for 24 h. Subsequently, mRNA was isolated and quantitative real-time PCR was conducted as described in Material and methods. Two distinct FPR1 **TaqMan** probes were applied: Hs04235426_s1 (**a** and **b**) and Hs01912307_s1 (**c** and **d**). Data were calculated as $2^{-\Delta\Delta C(T)}$ values normalized to the housekeeping genes ACTB and GUSB with unstimulated cells (control) serving as reference. Results are expressed as means ± SEM from three different experiments performed in duplicates. Statistical significance was calculated using one-way ANOVA followed by Dunnett's multiple comparison test with control cells serving as reference (***$p < 0.001$, **$p < 0.01$, and *$p < 0.05$). Please note the different scales of the *y*-axes

Comparison of potencies and efficacies of HA and H_2R agonists from cAMP accumulation, fMLP-induced $[Ca^{2+}]_i$, and FPR expression

We examined pairwise comparisons of potencies and efficacies of HA and H_2R agonists determined by cAMP accumulation, fMLP-induced $[Ca^{2+}]_i$, and FPR expression assays (Fig. 9a–f). Linear correlation would be indicated by an r^2 value of 1.00. Potencies of H_2R agonists were comparable to each other in all three assays (r^2 = 0.81, 0.86, 0.81) and increased as follows: 5-MHA < HA < AM < IM < UR-NK22. Unfortunately, concentration-response curves of DI in the cAMP and fMLP-induced $[Ca^{2+}]_i$ assays did not achieve saturation, and, consequently, DI had to be excluded from further examinations. Strikingly, efficacies of H_2R agonists were similar in fMLP-induced $[Ca^{2+}]_i$ and FPR expression (r^2 = 0.91). By contrast, efficacies in cAMP accumulation and fMLP-induced $[Ca^{2+}]_i$ (r^2 = 0.14) or FPR expression assay (r^2 = 0.20) differed markedly. Additionally, slopes of linear regression lines were shallower and deviated from the dashed lines representing identical values of efficacies.

Discussion

Since the H_2R canonically couples to G_s proteins, the determination of the second messenger cAMP is an appropriate standard method to study the pharmacological profile of this receptor (Seifert et al. 2013). Previous studies already used U937 promonocytes to investigate H_2R-mediated changes in cAMP concentrations (Gespach et al. 1985, Shayo et al. 1997, Smit et al. 1994). In our present study, we compared potencies and efficacies of HA and four well-established low-molecular H_2R agonists with the novel dimeric H_2R agonist UR-NK22 (Kagermeier et al. 2015). The increased potency of carbamoylguanidine-type H_2R ligands such as UR-NK22 and related acylguanidines (Birnkammer et al. 2012), consisting of two pharmacophoric moieties linked through a

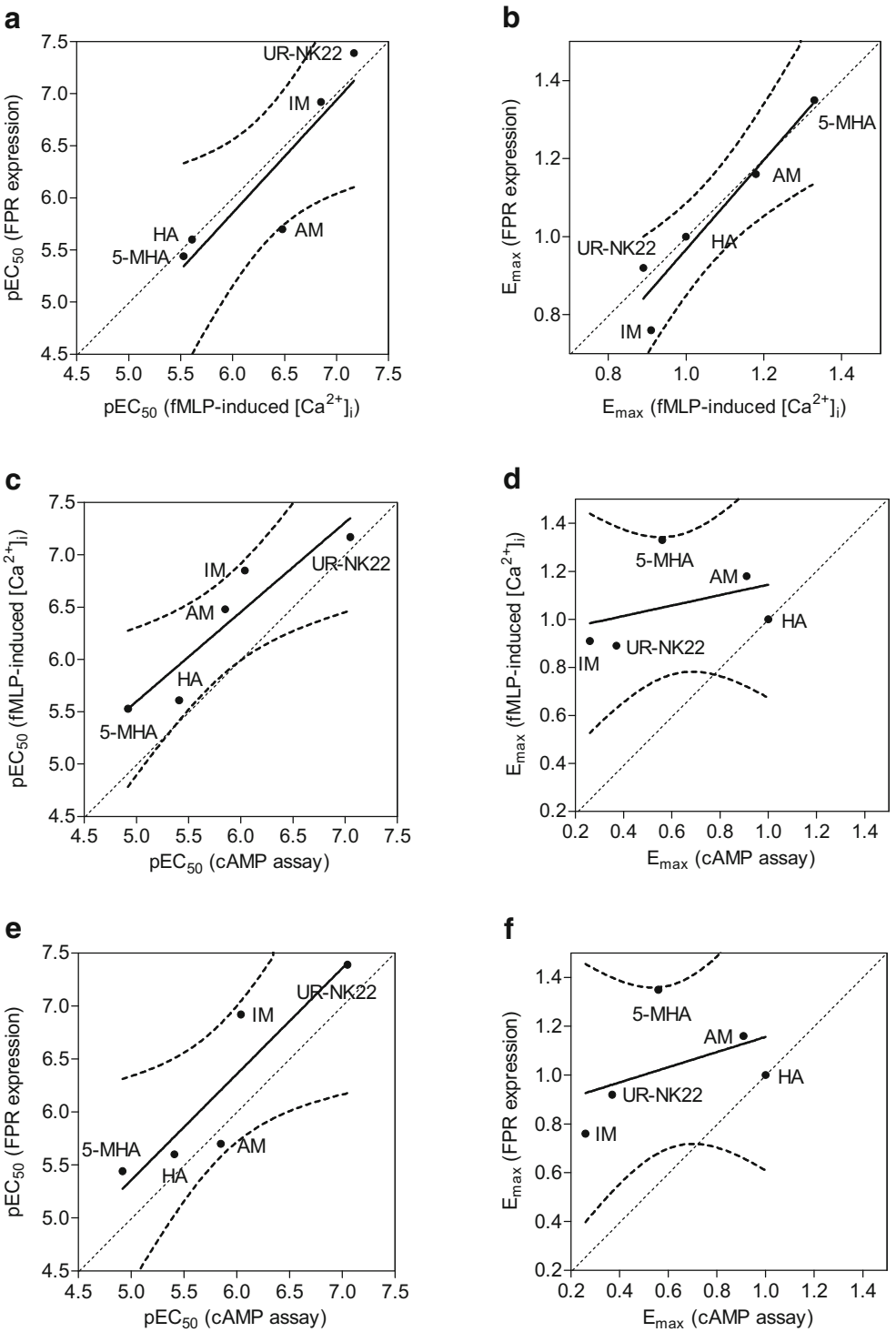

Fig. 9 Pairwise comparison of potencies (**a**, **c**, **e**) and efficacies (**b**, **d**, **f**) of HA and H_2R agonists calculated from cAMP accumulation, fMLP-induced $[Ca^{2+}]_i$, and FPR expression. Data from Table 1 were evaluated by linear regression analysis. The *diagonal dashed lines* illustrate identical values, whereas the *dashed lines surrounding the regression lines* represent the 95 % confidence intervals. **a** Slope, 1.084 ± 0.3007; r^2, 0.81. **b** Slope, 1.145 ± 0.2072; r^2, 0.91. **c** Slope, 0.8552 ± 0.1996; r^2, 0.86. **d** Slope, 0.2176 ± 0.3099; r^2, 0.14. **e** Slope, 1.000 ± 0.2775; r^2, 0.81. **f** Slope, 0.3107 ± 0.3589; r^2, 0.20

spacer, is most likely attributable to interaction with the orthosteric and an allosteric binding site at the same receptor protomer rather than simultaneous binding to the orthosteric sites of H_2R dimers (Birnkammer et al. 2012). UR-NK22 turned out to be the most potent but least effective agonist with respect to cAMP accumulation. These results correspond to our recently published data comparing the pharmacological profile of HA with that of UR-NK22 in human monocytes (Kagermeier et al. 2015). An increase of agonist potency relative to HA goes at the expense of efficacy.

Undifferentiated U937 promonocytes do not respond to chemotactic stimuli, but expression of chemoattractant receptors is induced during cell maturation (Fischer et al. 1980). Recently, Copsel et al. differentiated U937 cells with various

combinations of the H_2R agonist AM, ROL, and PROB for 72 h and, subsequently, determined cell maturation by expression of the C5a receptor (C5aR) via Western blot analysis as well as measurements of C5a-induced $[Ca^{2+}]_i$ with the Fura-2 AM method (Copsel et al. 2011). Like the FPR, the C5aR is a chemoattractant receptor coupling to pertussis toxin-sensitive G_i proteins and activation leads to increases in $[Ca^{2+}]_i$ (Snyderman and Goetzl 1981, Vanek et al. 1994). In our present study, we investigated expression of the FPR in order to assess U937 cell differentiation. Chaplinski and Niedel identified the FPR being rapidly expressed on the cell surface of HL-60 promyelocytes upon exposure to DB-cAMP (500 μM) within 2 h. Whereas more than 95 % of HL-60 cells already expressed the FPR after 24 h, morphological changes appeared later (Chaplinski and Niedel 1982). Kay et al. demonstrated FPR expression in U937 cells treated with DB-cAMP (1 mM) for 24 h (Kay et al. 1983). Our results are in accordance with the results of Copsel et al., who measured the largest changes in $[Ca^{2+}]_i$ caused by C5aR expression after co-treatment with AM, ROL, and PROB in U937 cells (Copsel et al. 2011). Because U937 cell maturation was only evaluated upon treatment with a fixed concentration of AM (10 μM), we extended the previous approach and analyzed HA as well as various selective H_2R agonists in the presence of IBMX and PROB. Additionally, in accordance with Copsel et al., PROB did not potentiate the effect of HA with respect to $cAMP_{intra}$ after exposure for 10 min, but provided an additive effect during cell maturation already after 24 h.

Our data show that incubation of U937 cells with HA or H_2R agonists in the presence of IBMX and PROB for 24 h were sufficient to induce FPR expression. In addition to functional assays such as fMLP-induced calcium mobilization (Cowen et al. 1991, Seifert et al. 1992), FPR expression can be evaluated directly either by fluorescently labeled ligands, such as fNleLFNleYK-FI (Schneider et al. 2012, Sklar et al. 1981), or by radioligands, such as [^{3}H]fMLP (Kay et al. 1983). However, application of [^{3}H]fMLP has become very costly since it is no longer available as regular catalog product, but has to be purchased as expensive custom-synthesis product. In this paper, we assessed FPR expression on U937 promonocytes both by fMLP-induced changes in $[Ca^{2+}]_i$ and fNleLFNleYK-FI binding. Both methods were sufficiently sensitive to allow the generation of concentration-response curves of HA and H_2R agonists with comparable potencies and efficacies. In conclusion, we identified the flow cytometric analysis as a highly suitable alternative to evaluate the induced FPR expression.

So far, induction of FPR expression during cell maturation was predominantly studied at the protein level by radioligand binding or binding of a fluorescently labeled FPR ligand (Chaplinski and Niedel 1982, Fischer et al. 1980, Kay et al. 1983). Perez et al. (1992) studied FPR expression both at the protein level by using the radioligand [^{125}I]-*N*-formyl-Nle-Leu-Phe-Tyr and at the mRNA level by northern blot analysis in DB-cAMP-stimulated HL-60 promyelocytes. To our knowledge, we are the first to characterize FPR expression at the mRNA level during cell maturation of U937 cells. Generally, co-treatment with different combinations of HA, PROB, and IBMX resulted in comparable effects on fMLP-induced changes in $[Ca^{2+}]_i$ and FPR expression at the mRNA level (Figs. 4 and 8). However, we have no explanation for the high induction of FPR mRNA expression by PROB alone or in combination with HA. Furthermore, we analyzed the influence of different concentrations of HA or H_2R agonists on FPR mRNA expression (Supplemental Fig. S1). Here, we noticed concentration-dependent increases in FPR mRNA levels as already described for DB-cAMP in HL-60 cells (Perez et al. 1992), but differences in day-to-day reproducibility hindered us from generating concentration-response curves. Consequently, direct comparison of potencies and efficacies calculated from fMLP-induced calcium mobilization or fNleLFNleYK-FI-binding with FPR mRNA expression was not possible.

Quantitative real-time PCR constitutes a sensitive method to study RNA expression, and we did our best to obtain reproducible data. To obtain RNA of equal quality in each experiment, we used the NucleoSpin RNA II Kit (Machery-Nagel, Düren, Germany) for RNA isolation and purified RNA was digested with DNase to remove contaminating genomic DNA. We normalized FPR1 expression to the two housekeeping genes ACTB and GUSB, which showed constant C_T (C_T = cycle threshold) values in each experiment (data of different concentrations of HA and H_2R agonists normalized to ACTB are not shown) (Bollmann et al. 2012, Udvardi et al. 2008). Furthermore, we analyzed FPR1 mRNA expression with two distinct FPR1 TaqMan probes, which bind to different domains on the mRNA of the FPR1 gene. However, relative quantification of FPR1 mRNA expression revealed up to 10-fold deviations between the two FPR1 TaqMan probes.

Assuming that the H_2R exclusively couples to G_s proteins, one would expect that FPR expression via H_2R is directly caused by cAMP generation. Here, we observed considerable discrepancies between efficacies of H_2R agonists in cAMP accumulation and FPR expression indicating that not only generation of cAMP is responsible for FPR expression via H_2R but that additional pathway(s) are activated when targeting the H_2R on U937 cells. Therefore, our study supports the concept of functional selectivity (Seifert 2013). There has already been important evidence for functional selectivity of the H_2R in the past. In the early 1990s, one of the authors (RS) already reported on dissociations between cAMP generation and increases in $[Ca^{2+}]_i$ caused by H_2R agonists in HL-60 promyelocytes (Seifert et al. 1992). Originally, these ligand-specific differences in signaling pathways were thought to be based on different H_2R subtypes, but there is

no evidence for functionally distinct H_2R subtypes in human myeloid cells (Reher et al. 2012). Furthermore, Gespach et al. explored cell type-specific differences in cAMP accumulation. In their study, the H_2R agonist impromidine (IM) acted not only as partial agonist in HL-60 promyelocytes but also as full agonist in human neutrophils (Gespach et al. 1982). These findings are consistent with our data. Here, we revealed lower efficacies of IM and UR-NK22 compared to HA in cAMP generation, whereas efficacies of both ligands were similar to HA in fMLP-induced $[Ca^{2+}]_i$ as well as FPR expression. Recently, we observed noncanonical H_2R signaling in human eosinophils, neutrophils, and monocytes with respect to cAMP accumulation and inhibition of fMLP-induced ROS generation. Additionally, we detected cell type-specific functional selectivity of the H_2R (Reher et al. 2012, Werner et al. 2014b). Furthermore, Alonso et al. reported on differing efficacies of H_2R ligands in cAMP generation and ERK1/2 phosphorylation in H_2R-transfected human embryonic kidney 293T (HEK293T) cells (Alonso et al. 2014).

Assessment of FPR expression with the fluorescently labeled ligand fNleLFNleYK-FI provides a new approach to study the pharmacological profile of the H_2R. Since the early 1970s, the positive chronotropic response of the isolated spontaneously beating guinea pig right atrium to H_2R ligands has been a frequently used assay (Birnkammer et al. 2012, Black et al. 1972, Ghorai et al. 2008, Reinhardt et al. 1974, Smit et al. 1994). Unfortunately, these experiments demand a large number of animals which is time-consuming and costly. In addition, ever-increasing restrictions of animal protection laws call for the search of alternative systems. Besides, species selectivity of the H_2R has to be taken into account when translating results of a nonhuman biological system to the human one (Strasser et al. 2013). Moreover, a well-established system to analyze new ligands is Sf9 insect cell membranes expressing the recombinant H_2R of various species (Birnkammer et al. 2012, Kelley et al. 2001, Preuss et al. 2007). Advantageously, Sf9 cells lack endogenous histamine receptor expression; thus, effects caused by other H_xR subtypes can be excluded. However, [^{3}H]TIO binding, [^{35}S]GTPγS binding or [^{32}P]GTPase assays require working with radioactive material, which is getting more and more difficult due to legal restrictions. Furthermore, eosinophils, neutrophils, and monocytes can be purified from human peripheral blood to study H_2R ligands (Reher et al. 2012, Werner et al. 2014b). Disadvantageously, a limited number of cells, specifically with regard to monocytes and eosinophils, impede screening of compound libraries. Moreover, studying myeloid cells depends on volunteers to donate blood and inter-individual variability renders data analysis more difficult (Brunskole Hummel et al. 2013, Werner et al. 2014b). Therefore, human cell culture systems should be preferably used to assess the pharmacological profile of the H_2R. In U937 promonocytes, for example, concentration-dependent generation of the second messenger cAMP was determined due to stimulation with H_2R agonists (Gespach et al. 1985, Shayo et al. 1997, Smit et al. 1994). Additionally, changes in $[Ca^{2+}]_i$ caused by H_2R agonists were recorded in HL-60 promyelocytes (Seifert et al. 1992). Furthermore, HEK293T cells that do not endogenously express H_xR subtypes can be transfected with the H_2R of the species of interest (Alonso et al. 2014). A list of representative publications studying the pharmacological profile of H_2R ligands is depicted in Table 2.

In conclusion, we pharmacologically characterized the H_2R with HA and five selective H_2R ligands with respect to

Table 2 Representative systems used for the pharmacological analysis of the H_2R

Biological system	Methods	References
HL-60 promyelocytes	$[Ca^{2+}]_i$ (Fura-2 AM method)	(Seifert et al. 1992)
U937 promonocytes	cAMP (radioligand binding assay [^{3}H]cAMP)	(Shayo et al. 1997, Smit et al. 1994)
	cAMP (radioimmunoassay [^{125}I] tyrosylsuccinyl-cAMP + antibody 301–8)	(Gespach et al. 1985)
Human neutrophils and eosinophils	ROS (cytochrome C assay), cAMP (HPLC-MS/MS)	(Reher et al. 2012)
Human neutrophils	cAMP (radioimmunoassay [^{125}I] tyrosylsuccinyl-cAMP + antibody 301–8)	(Gespach and Abita 1982)
Human monocytes	ROS (chemiluminescence assay), cAMP (HPLC-MS/MS)	(Werner et al. 2014b)
H_2R-transfected HEK293T cells	cAMP (radioligand binding assay [^{3}H]cAMP)	(Alonso et al. 2014)
Sf9 insect cell membranes expressing recombinant H_2R	GTPase assay ([γ-^{32}P]GTP)	(Kelley et al. 2001, Preuss et al. 2007)
	[^{35}S]GTPγS binding study	(Birnkammer et al. 2012, Kelley et al. 2001)
	[^{3}H]TIO binding study	(Kelley et al. 2001)
	[^{3}H]UR-DE257 binding study	(Baumeister et al. 2015)
Guinea pig (right atrium)	Positive chronotropic response	(Birnkammer et al. 2012, Black et al. 1972, Ghorai et al. 2008, Smit et al. 1994)

cAMP accumulation and FPR expression in U937 cells. We revealed FPR expression both at the mRNA and the protein level during U937 cell maturation. We identified the bivalent ligand UR-NK22 as the most potent agonist compared to the low-molecular H_2R agonists and, therefore, as an interesting pharmacological tool for future investigations of the H_2R. Moreover, discrepancies between cAMP generation and FPR expression point to functional selectivity of the H_2R. Most importantly, the flow cytometric analysis of FPR expression provides a rapid, simple, sensitive, inexpensive, and reliable method to study H_2R pharmacology, which neither requires radioactive material nor human blood cells nor animal models.

Acknowledgments We thank Mrs. A. Garbe (Research Core Unit Metabolomics, Hannover Medical School) for performing the HPLC-MS/MS analyses. Many thanks also go to Mrs. N. Kagermeier (Institute of Pharmacy, University of Regensburg) for the synthesis of UR-NK22, which was supported by the Graduate Training Program (Graduiertenkolleg) GRK1910 of the Deutsche Forschungsgemeinschaft. Thanks are also due to the reviewers for their helpful critique.

References

Alonso N, Monczor F, Echeverria E, Davio C, Shayo C, Fernandez N (2014) Signal transduction mechanism of biased ligands at histamine H_2 receptors. Biochem J 459:117–126

Azzi M, Charest PG, Angers S, Rousseau G, Kohout T, Bouvier M, Pineyro G (2003) β-arrestin-mediated activation of MAPK by inverse agonists reveals distinct active conformations for G protein-coupled receptors. Proc Natl Acad Sci U S A 100:11406–11411

Baumeister P, Erdmann D, Biselli S, Kagermeier N, Elz S, Bernhardt G, Buschauer A (2015) [^{3}H]UR-DE257: development of a tritium-labeled squaramide-type selective histamine H_2 receptor antagonist. ChemMedChem 10:83–93

Birnkammer T, Spickenreither A, Brunskole I, Lopuch M, Kagermeier N, Bernhardt G, Dove S, Seifert R, Elz S, Buschauer A (2012) The bivalent ligand approach leads to highly potent and selective acylguanidine-type histamine H_2 receptor agonists. J Med Chem 55:1147–1160

Black JW, Duncan WA, Durant CJ, Ganellin CR, Parsons EM (1972) Definition and antagonism of histamine H_2-receptors. Nature 236: 385–390

Bollmann F, Casper I, Henke J, Pautz A (2012) qRT-PCR: a method and its difficulties. Naunyn Schmiedeberg's Arch Pharmacol 385:949–951

Brodsky A, Davio C, Shayo C, Lemos Legnazzi B, Barbosa M, Lardo M, Morelli A, Baldi A, Sanchez Avalos JC, Rivera E (1998) Forskolin induces U937 cell line differentiation as a result of a sustained cAMP elevation. Eur J Pharmacol 350:121–127

Brunskole Hummel I, Reinartz MT, Kalble S, Burhenne H, Schwede F, Buschauer A, Seifert R (2013) Dissociations in the effects of β_2-adrenergic receptor agonists on cAMP formation and superoxide production in human neutrophils: support for the concept of functional selectivity. PLoS One 8:e64556

Chaplinski TJ, Niedel JE (1982) Cyclic nucleotide-induced maturation of human promyelocytic leukemia cells. J Clin Invest 70:953–964

Copsel S, Garcia C, Diez F, Vermeulem M, Baldi A, Bianciotti LG, Russel FG, Shayo C, Davio C (2011) Multidrug resistance protein 4 (MRP4/ABCC4) regulates cAMP cellular levels and controls human leukemia cell proliferation and differentiation. J Biol Chem 286:6979–6988

Cowen DS, Berger M, Nuttle L, Dubyak GR (1991) Chronic treatment with P_2-purinergic receptor agonists induces phenotypic modulation of the HL-60 and U937 human myelogenous leukemia cell lines. J Leukoc Biol 50:109–122

Fechner GA, Jacobs JJ, Parsons PG (1994) Dimaprit analogues inhibit tyrosinase via a disulphide breakdown product independently of the histamine H_2 receptor. Biochem Biophys Res Commun 201:687–693

Fischer DG, Pike MC, Koren HS, Snyderman R (1980) Chemotactically responsive and nonresposive forms of a continuous human monocyte cell line. J Immunol 125:463–465

Gespach C, Abita JP (1982) Human polymorphonuclear neutrophils. Pharmacological characterization of histamine receptors mediating the elevation of cyclic AMP. Mol Pharmacol 21:78–85

Gespach C, Saal F, Cost H, Abita JP (1982) Identification and characterization of surface receptors for histamine in the human promyelocytic leukemia cell line HL-60. Comparison with human peripheral neutrophils. Mol Pharmacol 22:547–553

Gespach C, Cost H, Abita JP (1985) Histamine H_2 receptor activity during the differentiation of the human monocytic-like cell line U-937. Comparison with prostaglandins and isoproterenol. FEBS Lett 184: 207–213

Ghorai P, Kraus A, Keller M, Gotte C, Igel P, Schneider E, Schnell D, Bernhardt G, Dove S, Zabel M, Elz S, Seifert R, Buschauer A (2008) Acylguanidines as bioisosteres of guanidines: N^G-acylated imidazolylpropylguanidines, a new class of histamine H_2 receptor agonists. J Med Chem 51:7193–7204

Grynkiewicz G, Poenie M, Tsien RY (1985) A new generation of Ca^{2+} indicators with greatly improved fluorescence properties. J Biol Chem 260:3440–3450

Hershcovici T, Fass R (2011) Gastro-oesophageal reflux disease: beyond proton pump inhibitor therapy. Drugs 71:2381–2389

Kagermeier N, Werner K, Keller M, Baumeister P, Bernhardt G, Seifert R, Buschauer A (2015) Dimeric carbamoylguanidine-type histamine H_2 receptor ligands: a new class of potent and selective agonists. Bioorg Med Chem. doi:10.1016/j.bmc.2015.1001.1012

Kay GE, Lane BC, Snyderman R (1983) Induction of selective biological responses to chemoattractants in a human monocyte-like cell line. Infect Immun 41:1166–1174

Kelley MT, Burckstummer T, Wenzel-Seifert K, Dove S, Buschauer A, Seifert R (2001) Distinct interaction of human and guinea pig histamine H_2-receptor with guanidine-type agonists. Mol Pharmacol 60: 1210–1225

Kenakin TP (2012) Biased signalling and allosteric machines: new vistas and challenges for drug discovery. Br J Pharmacol 165:1659–1669

Livak KJ, Schmittgen TD (2001) Analysis of relative gene expression data using real-time quantitative PCR and the $2(-\Delta\Delta C_T)$ method. Methods 25:402–408

Martner A, Thoren FB, Aurelius J, Soderholm J, Brune M, Hellstrand K (2010) Immunotherapy with histamine dihydrochloride for the prevention of relapse in acute myeloid leukemia. Expert Rev Hematol 3:381–391

Perez HD, Kelly E, Holmes R (1992) Regulation of formyl peptide receptor expression and its mRNA levels during differentiation of HL-60 cells. J Biol Chem 267:358–363

Preuss H, Ghorai P, Kraus A, Dove S, Buschauer A, Seifert R (2007) Constitutive activity and ligand selectivity of human, guinea pig, rat, and canine histamine H_2 receptors. J Pharmacol Exp Ther 321:983–995

Reher TM, Brunskole I, Neumann D, Seifert R (2012) Evidence for ligand-specific conformations of the histamine H_2-receptor in human eosinophils and neutrophils. Biochem Pharmacol 84:1174–1185

Reinhardt D, Wagner J, Schumann HJ (1974) Differentiation of H_1- and H_2-receptors mediating positive chrono- and inotropic responses to histamine on atrial preparations of the guinea-pig. Agents Actions 4: 217–221

Sawutz DG, Kalinyak K, Whitsett JA, Johnson CL (1984) Histamine H_2 receptor desensitization in HL-60 human promyelocytic leukemia cells. J Pharmacol Exp Ther 231:1–7

Schneider EH, Weaver JD, Gaur SS, Tripathi BK, Jesaitis AJ, Zelenka PS, Gao JL, Murphy PM (2012) The leukocyte chemotactic receptor FPR1 is functionally expressed on human lens epithelial cells. J Biol Chem 287:40779–40792

Seifert R (2013) Functional selectivity of G-protein-coupled receptors: from recombinant systems to native human cells. Biochem Pharmacol 86:853–861

Seifert R, Hoer A, Schwaner I, Buschauer A (1992) Histamine increases cytosolic Ca^{2+} in HL-60 promyelocytes predominantly via H_2 receptors with an unique agonist/antagonist profile and induces functional differentiation. Mol Pharmacol 42:235–241

Seifert R, Strasser A, Schneider EH, Neumann D, Dove S, Buschauer A (2013) Molecular and cellular analysis of human histamine receptor subtypes. Trends Pharmacol Sci 34:33–58

Shayo C, Davio C, Brodsky A, Mladovan AG, Legnazzi BL, Rivera E, Baldi A (1997) Histamine modulates the expression of c-fos through cyclic AMP production via the H_2 receptor in the human promonocytic cell line U937. Mol Pharmacol 51:983–990

Sklar LA, Oades ZG, Jesaitis AJ, Painter RG, Cochrane CG (1981) Fluoresceinated chemotactic peptide and high-affinity antifluorescein antibody as a probe of the temporal characteristics of neutrophil stimulation. Proc Natl Acad Sci U S A 78:7540–7544

Smit MJ, Leurs R, Shukrula SR, Bast A, Timmerman H (1994) Rapid desensitization of the histamine H_2 receptor on the human monocytic cell line U937. Eur J Pharmacol 288:17–25

Snyderman R, Goetzl EJ (1981) Molecular and cellular mechanisms of leukocyte chemotaxis. Science 213:830–837

Strasser A, Wittmann HJ, Buschauer A, Schneider EH, Seifert R (2013) Species-dependent activities of G-protein-coupled receptor ligands: lessons from histamine receptor orthologs. Trends Pharmacol Sci 34:13–32

Udvardi MK, Czechowski T, Scheible WR (2008) Eleven golden rules of quantitative RT-PCR. Plant Cell 20:1736–1737

Urban JD, Clarke WP, von Zastrow M, Nichols DE, Kobilka B, Weinstein H, Javitch JA, Roth BL, Christopoulos A, Sexton PM, Miller KJ, Spedding M, Mailman RB (2007) Functional selectivity and classical concepts of quantitative pharmacology. J Pharmacol Exp Ther 320:1–13

Vanek M, Hawkins LD, Gusovsky F (1994) Coupling of the C5a receptor to G_i in U-937 cells and in cells transfected with C5a receptor cDNA. Mol Pharmacol 46:832–839

Wenzel-Seifert K, Hurt CM, Seifert R (1998) High constitutive activity of the human formyl peptide receptor. J Biol Chem 273:24181–24189

Werner K, Neumann D, Buschauer A, Seifert R (2014a) No evidence for histamine H_4 receptor in human monocytes. J Pharmacol Exp Ther 351:519–526

Werner K, Neumann D, Seifert R (2014b) Analysis of the histamine H_2-receptor in human monocytes. Biochem Pharmacol 92:369–379